Journal of Colloid and Interface Science 555 (2019) 245–253

Contents lists available at ScienceDirect

Journal of Colloid and Interface Science

journal homepage: www.elsevier.com/locate/jcis

Regular Article

Adhesion force measurements on functionalized microbeads: An in-depth comparison of computer controlled micropipette and fluidic force microscopy

Tamás Gerecsei [a,b,*], István Erdődi [c], Beatrix Peter [a], Csaba Hős [c], Sándor Kurunczi [a], Imre Derényi [b], Bálint Szabó [b], Robert Horvath [a]

[a] Nanobiosensorics Group, Institute for Technical Physics and Materials Science, Centre for Energy Research, Hungarian Academy of Sciences, Budapest, Hungary
[b] Department of Biological Physics, Eötvös University, Budapest, Hungary
[c] Department of Hydrodynamic Systems, Budapest University of Technology and Economics, Budapest, Hungary

GRAPHICAL ABSTRACT

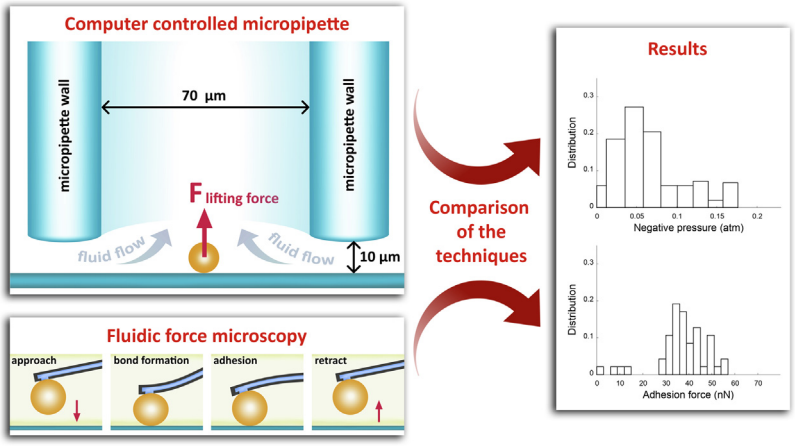

ARTICLE INFO

Article history:
Received 24 June 2019
Revised 29 July 2019
Accepted 30 July 2019
Available online 31 July 2019

ABSTRACT

Characterization of the binding of functionalized microparticles to surfaces with a specific chemistry sheds light on molecular scale interactions. Polymer or protein adsorption are often monitored by colloid particle deposition. Force measurements on microbeads by atomic force microscopy (AFM) or optical tweezers are standard methods in molecular biophysics, but typically have low throughput. Washing and centrifuge assays with (bio)chemically decorated microbeads provide better statistics, but only qualitative results without a calibrated binding force or energy value. In the present work we demonstrate that a computer controlled micropipette (CCMP) is a straightforward and high-throughput alternative to quantify the surface adhesion of functionalized microparticles. However, being an indirect force measurement technique, its in-depth comparison with a direct force measurement is a prerequisite of applications requiring calibrated adhesion force values. To this end, we attached polystyrene microbeads to a solid support by the avidin-biotin linkage. We measured the adhesion strength of the microbeads with both a specialized robotic fluid force microscope (FluidFM BOT) and CCMP. Furthermore, the

Abbreviations: AFM, atomic force microscopy; bar, 100,000 Pa; mbar, 100 Pa; CCMP, computer controlled micropipette; OWLS, optical waveguide lightmode spectroscopy; CCD, charge coupled device; FluidFM, fluidic force microscopy; PLL, poly-L-lysine; PEG, poly ethylene glycol; PLL-g-PEG, poly-L-lysine grafted poly ethylene glycol.

* Corresponding author.
E-mail address: gerecsei.tamas@mfa.kfki.hu (T. Gerecsei).

https://doi.org/10.1016/j.jcis.2019.07.102

bead-support contact zone was directly characterized on an optical waveguide biosensor to determine the density of avidin molecules. Distribution of the detachment force recorded on ~50 individual beads by FluidFM BOT was compared to the adhesion distribution obtained from CCMP measurements on hundreds of individual beads. We found that both methods provide unimodal histograms. We conclude that FluidFM BOT can directly measure the detachment force curve of 50 microbeads in 150 min. CCMP can provide calibrated binding/adhesion force values of 120 microbeads in an hour.

1. Introduction

The adhesion of microparticles to specific surfaces is a general problem in surface and colloid sciences with a relevance in a wide range of fields. A number of industrial process such as printing [1], steel polishing [2] and polymer surface coating involves an interaction between micrometer sized particles and flat surfaces. In paper making the adhesion between cellulose and silica microparticles is of interest for controlling the production process and understanding flocculation [3]. Measuring the adhesion force generated by certain surface-adsorbed polymers is important for applications such as the stabilization of suspensions, biomedical implants and industrial coatings [4]. Colloid particle deposition is a general method to characterize surface interaction between adsorbed protein layers through the observation of particle attachment to a surface [5]. Humidity [6], surface roughness [7], the presence of specific solutes in an aqueous environment [8] as well as several other parameters can influence microparticle adhesion processes, which calls for simple and effective techniques for their measurement. Despite its importance a high throughput and sensitive method to characterize microbead adhesion with an extensive force range is still missing.

The adhesion of living cells (that can be regarded as a special type of microparticles) has been of great interest in biological sciences due to its importance in key processes such as tissue formation and development. Cell adhesion itself is a substantially complex active biological process involving signalization pathways [9], numerous adhesion proteins [10] and further structures such as glycocalix [11] elements. Traditional methods for measuring cell adhesion rely on population averaging, however modern advances in cellular biology point to the fact that exploring population inhomogeneity is crucial for understanding *in vivo* tissue function and creating novel therapeutic and diagnostic methods [12].

One of the early techniques for the measurement of microparticle adhesion (including cells) is the shear stress generating washing assay, where a laminar fluid flow parallel to the surface is applied to the adhered particles and the fraction of the microparticle population remaining attached to the surface is measured. While these methods are relatively easy to execute, they lack the possibility of calibrated force measurements. Similarly, centrifuge based methods have been developed to detach a fraction of the particles, depending on the adhesion strength between them and the surface [13,14]. Although this method can characterize the overall effect of surface coatings in some cases [15,16], its widespread application is hindered by certain drawbacks, most importantly the limited force range and inaccurate force characterization [17,18]. Furthermore, both shear flow and centrifuge-based methods measure the population average of the adhesion force of particles without the capability to target individual beads or cells.

In recent years acoustic force spectroscopy (AFS), a method using acoustic waves to manipulate surface attached single cells and beads has been developed and applied in several studies [19,20]. In these experiments, acoustic waves were applied in a measurement chamber to lift up beads from a surface. This way one can stretch single DNA or other polymer strands in a precisely controlled manner as well as probe the adhesion force between living cells. While this method can achieve high throughput by measuring a large number of beads at the same time, the available force range is limited to under 15 nN [21]. Moreover, the perquisite for AFS calibration is a homogenous shape distribution which hinders the measurement of spread out, irregularly shaped cells [22].

Colloid force spectroscopy is a well-established method to quantify microbead adhesion [4]. It applies atomic force microscopy (AFM) to record the force-distance curves of the interaction of the beads and a planar surface. The measured particle is immobilized on the tip of the AFM cantilever by application of an adhesive coating. Similar techniques, such as the surface force apparatus [23,24] and AFM tip functionalization [25–27] have been successfully used to explore the structure of noncovalent molecular bonds. Using high speed force spectroscopy Rico et al. [28] were able to map the loading rate-dependent unbinding pathways of the streptavidin-biotin bond emphasizing the highly complex energy landscape that a single binding pocket can exhibit.

In spite of the impressive advances of force spectroscopy, the throughput of most methods is insufficient for collecting data from a large population of particles or cells. Typically, the throughput of these techniques is limited to 5–10 measurements per day, being a strong limitation of in-depth characterization. The limiting factor is the time-consuming functionalization of the AFM tip as well as the limited range of movement of the probe making it impossible to cover sample areas of several square centimeters. Furthermore, most techniques focus on the measurement of single molecular bonds and cannot be readily adapted for the probing of microparticle adhesion with several hundreds or thousands of adhesive molecules.

A significant development to overcome these challenges has been the introduction of fluidic force microscopy (FluidFM) [29]. This novel technology is based on AFM cantilevers with an incorporated microfluidic channel ending in an aperture at the tip. The other end of the fluid filled channel is connected to a pressure controller unit. By applying a negative pressure to the channel, the cantilever tip can grab the microparticle eliminating the need for time consuming immobilization procedures. Using FluidFM, the exchange of the colloid or microparticles becomes trivial as a positive pressure in the channel removes the particle from the aperture, after which the next bead can be readily attached [30]. It increases the throughput of measurements by an order of magnitude. Helfricht et al. [31] demonstrated that the interaction of beads as small as 500 nm can be evaluated by FluidFM opening the possibility for measurements in the colloid particle size range. FluidFM is also applicable for live cell adhesion measurements, however, the throughput remains limited by unspecific binding of cells to the cantilever and the resulting clogging. An important development was the introduction of the FluidFM BOT technology, where the fluid force measurements and manipulations can be performed on mm-cm scale areas in a completely automatized manner [32], further increasing the throughput of this powerful technology

In the present work we introduce a novel method for the measurement of the binding/adhesion force of microbeads, based on a

computer controlled micropipette (CCMP), potentially offering even larger throughput and upper force limit in an automatized manner. In our setup, a glass microcapillary is automatically positioned above the beads recognized by computer vision. The micropipette probes their adhesion to the surface by the application of a negative pressure. This negative pressure between the inside of the micropipette and the environment results in an upwards flow that exerts a hydrodynamic lifting force on the bead. In order to attain an accurate calibration of the hydrodynamic force acting on the particle, we devised a model system based on 10 μm biotinylated polystyrene beads attached to a polymer-functionalized glass surface through an avidin crosslinker. The noncovalent bond between the small organic molecule biotin (vitamin A) and the 66 kDa protein avidin is the strongest known non-covalent bond found in biological systems. It has been extensively studied and became a standard biochemical immobilization technique due to the possibility of covalently binding biotin to a number of different molecules and surfaces. We successfully applied the data acquired by optical waveguide lightmode spectroscopy (OWLS) to measure the avidin density on the functionalized surface. We used FluidFM BOT to directly measure the adhesion force of 47 individual beads. Detachment of hundreds of microparticles was measured by CCMP and the adhesion spectrum was compared to the one measured by FluidFM. The peaks of the histograms were correlated with each other to interpret the negative pressure measured by the micropipette. Such calibration of the CCMP enables the applications of this method in the field of molecular biophysics for high-throughput nanonewton scale microparticle binding/adhesion force assays. FluidFM BOT proved to be a high-throughput direct force measurement apparatus for characterizing functionalized microbead binding thus calibrating indirect force measurements.

2. Materials and methods

2.1. Functionalized beads and surfaces

All chemicals used were analytical grade unless otherwise stated. 4-(2-hydroxyethyl)–1-piperazine ethanesulfonic acid (HEPES), from Merck (Germany) was applied as assay buffer, dissolved in Milli-Q water (with resistivity of 18 MΩ cm) to 10 mM and set to pH 7.4. Avidin from egg white was purchased from VWR (Hungary) and aliquots were stored at −20 °C until use. 0.25 mg/ml avidin was dissolved in 10 mM HEPES buffer at pH 7.4 and applied in the experiments. The biotinylated synthetic copolymer, poly(L-lysine)-*graft*-poly(ethylene glycol) (PLL-*g*-PEG), with the architecture of PLL(20)-g[3.5]-PEG(2)/PEG(3.4)-biotin with 50% of side-chains biotinylated was obtained in its powder form from SuSoS AG (Switzerland). The molecular weight of the PLL backbone and the PEG chains were 20 kDa and 2 kDa respectively and the grafting density [(lysine-mers)/(PEG side chains)] was 3.4. Polystyrene biotinylated bead solution with a solid concentration of 1% and an average bead diameter of d = 10 μm was purchased from Nanocs (USA), and stored at 4 °C until use.

2.2. Fluidic force microscopy (FluidFM)

Fluidic force microscopy (FluidFM) was performed using a standalone system FluidFM BOT commercialized by Cytosurge AG (Switzerland). Before the adhesion measurements, the FluidFM BOT Micropipette probe was placed into the device for calibration. Probes with an aperture diameter of 2 μm and a nominal spring constant of 0.2 N/m were filled up with 2 μl of HEPES buffer. A probe was mounted onto the head of the FluidFM and the laser was positioned at the end of the cantilever manually. Afterwards, the mirror reflecting the laser light to the CCD sensor was automatically adjusted to achieve optimal light distribution between the sensor parts. The spring constant was measured using the thermal vibration spectrum of the cantilever (Sader method [33]). Next, the probe was approached to the sample and the inverse optical lever sensitivity was measured by approaching the cantilever to the surface three times and fitting the deflection-displacement curve with a first order polynomial. The average of the three fitted slopes was accepted as the valid sensitivity (in m/V units). The adhesion force curves were calculated by multiplying the differential signal of the CCD sensor (mV) with the sensitivity then with the spring constant to change the distance values to force. The experiments presented here were done in colloid spectroscopy mode. A bead was detached from the surface using the probe, then it was fixed to its aperture by a negative pressure of - 700 mbar. The probe with the bead attached was then placed in contact with the surface for a certain amount of time (pause time), then retracted from the surface with a given speed (retraction speed). The process of the measurement is illustrated in Fig. 2(a). The following parameters were used for the measurements: pause time: 1 min, retraction speed: 1 μm/s, retraction distance 5 μm. For using 10 μm beads, the 2 μm aperture probe proved to be the most efficient.

2.3. Computer controlled micropipette (CCMP)

The adhesion of beads was analyzed with an imaging-based CCMP (CellSorter, Hungary). 35 mm glass bottom Petri dishes (Greiner, Hungary) were used in all experiments. To coat the dish surface, 0.5 mg/ml PLL-*g*-PEG-biotin dissolved in 10 mM HEPES was pipetted and incubated on a rocker for 30 min at room temperature. Afterwards, the dishes were washed two times with HEPES buffer and an avidin solution (0.25 mg/ml in 10 mM HEPES) was added to the dishes and incubated on a rocker for 30 min at room temperature. Subsequently, the dishes were washed two times with HEPES buffer again. Then the bead solution (2 μl 1% bead stock solution in 1 ml HEPES) was pipetted into the dishes. Part of the Petri dish was scanned by a motorized microscope (Zeiss Axio Observer Z1) equipped with a digital camera and saved as a region of interest (ROI). The scanned image was analyzed by the CellSorter software and the beads were automatically detected using a built-in algorithm [34,35]. The fastest possible path of the micropipette above the beads was also determined by the software in order to minimize measurement time. Afterwards, each bead was visited and probed by the micropipette through the application of a pre-set negative pressure. The glass micropipette with an aperture of 70 μm approached the bottom of the Petri dish to a distance of 10 ± 1 μm (Fig. 3(a)). To apply the negative pressure in the micropipette, a high-speed fluid valve connected to a syringe was opened for a pre-defined time (valve opening time) above each bead. The exact amount of this time can generally be adapted to the applications, in the present paper it is separately state for every measurement. After each cycle of the measurement the original area selected within the Petri dish was scanned again and the negative pressure value was manually adjusted to the next level. Subsequently each detected bead was probed again by the micropipette. This process was continued in six cycles. CellSorter software determined the coordinates of the beads by computer vision and saved them before and after each cycle. The bead coordinates before and after the cycles were compared to determine the ratio of the beads remaining on the surface.

2.4. Optical waveguide lightmode spectroscopy (OWLS)

Optical waveguide lightmode spectroscopy (OWLS) is a label-free surface-sensitive method using an evanescent electric field generated during total internal reflection of a laser light. First, an

optical waveguide sensor chip with and incorporated coupling grating is mounted onto the device (type OW2400, Microvacuum Ltd., Hungary). The illuminating laser beam is coupled into the chip and the OWLS instrument (BIOS210, Microvacuum Ltd., Hungary) records the effective refractive indices of the zeroth-order TE (transverse electric) and TM (transverse magnetic) polarized waveguide modes through the measurement of the coupling angle. The resolution of the acquisition is ~13 s. Upon biomolecule adsorption onto the surface of the sensor, the effective refractive indices shift to higher values, allowing monitoring of the in situ kinetics of adsorption processes. Prior to every experiment the waveguide sensor chips underwent a standard cleaning routine e.g. immersed into chromic acid (Merck, Germany) for 3 min, followed by rinsing with Milli-Q water, KOH and Milli-Q again. The chips were then placed into an ultrasonic bath for at least 30 min and the bathing Milli-Q water was changed in every 5 min. The cleaned waveguides were incubated in HEPES buffer overnight [36].

In the present study, we use this sensitive technique to reveal the subsequent adsorption kinetics of PLL-*g*-PEG-biotin, avidin and polystyrene biotinylated beads. First, the baseline was recorded with HEPES buffer (50 min), then PLL-*g*-PEG-biotin solution was injected and let to absorb for ~30 min, followed by washing with HEPES buffer for 40 min. Then the avidin solution was injected and let to absorb for 80 min and was again washed with HEPES buffer for 35 min. After that, the bead solution was injected and let to absorb for 70 min, followed by a washing step again with HEPES buffer for 40 min. During the washing steps, the buffer was pumped through the measurement cuvette with a speed of 1 μl/s using a peristaltic pump.

3. Results and discussions

3.1. Characterization of surface deposition of functionalized beads in situ by optical waveguide lightmode spectroscopy

In order to validate the adhesion force spectrum measured by CCMP, we used a reproducible, robust and widely applicable model system: 10 μm diameter biotinylated polystyrene beads adhered to an avidin-functionalized surface. The molecular structure of the system can be seen in Fig. 1(a). To gain quantitative information about the adhesion process of the microbeads, it was monitored in situ by optical waveguide lightmode spectroscopy (OWLS). This evanescent field based technique monitors the refractive index (RI) in the direct vicinity of the sensor chip [37–39] (Fig. 1(b)) and the surface adsorbed mass density can be also calculated in a straightforward manner. The surface density of the absorbed layers during the measurement can be seen in Fig. 1(c). The avidin layer is adsorbed in a surface mass density of 70 ng/cm^2. Fig. 1(d) shows a microscopy image of the sensor area after the beads have been introduced on the surface.

3.2. Detachment of beads using fluidic force microscopy – direct adhesion force measurements

To get an accurate characterization of the adhesion force distribution of the surface attached microbeads, fluidic force microscopy was used. Beads were picked up using −700 mbar negative pressure in the microfluidic channel of the cantilever. We needed to slightly jog the bead with the cantilever to pick it up by the

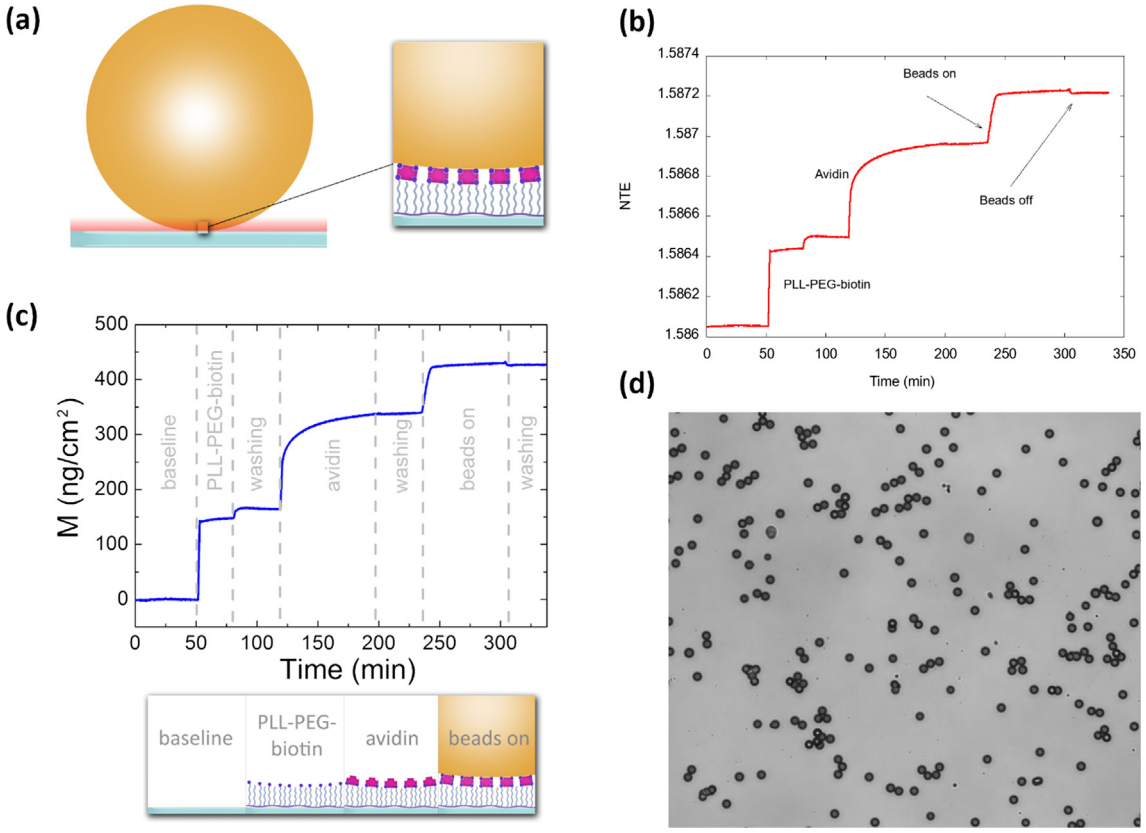

Fig. 1. (a) Illustration of the polystyrene bead (d = 10 μm) attached to the support. The red area shows the evanescent electric field of the OWLS. The PLL-*g*-PEG layer (blue chains) covalently grafted with biotin (blue circles) is adsorbed to the surface. The avidin crosslinker (purple boxes) attaches the biotinylated bead to the surface. (b) Effective refractive index change calculated from the TE mode (NTE) as a function of time during the buildup of the molecular layers. (c) The result of the OWLS measurement monitoring the assembly of the surface. The components are added to the measurement cuvette followed by subsequent washing cycles. The mass scale is calculated from the TE (transverse electric) signal. (d) Characteristic image showing the adhered beads on the surface of the OWLS chip. The coverage of beads is 9.37%. (For interpretation of the references to colour in this figure legend, the reader is referred to the web version of this article.)

negative pressure. A pickup was accepted only if the bead was visibly positioned below the middle of the aperture, otherwise the bead was removed and another one was picked up (Fig. 2(b)). Adhesion curves such as the ones in Fig. 2(c) were recorded by approaching the cantilever holding the bead to the surface, letting the bead adhere to the planar surface for 1 min, then retracting the cantilever with a speed of 1 μm/s.

The adhesion force values were extracted from the curves using the EDNA software provided by Cytosurge. The adhesion force of a bead is defined as the largest pulling force measured during the detachment event, which is the minimum of the adhesion curves. Typical adhesion curves are shown in Fig. 2(c). Curves showing the time-displacement data are demonstrated in Fig. S1. The histogram of the distribution of adhesion force values for N = 47 beads is shown in Fig. 2(d). The average adhesion force with the standard error of the mean is 36.65 ± 1.83 nN. The distribution is relatively compact with few outlier values. There is however an upper limit to the measureable detachment force determined by the contact force between the cantilever and the bead, which depends on the area of the aperture. In the experiments presented here this maximal force is 460 nN which stays far above the adhesion spectrum of the beads.

Dörig et al. [30] conducted experiments using a similar, PLL-*g*-PEG-biotin based system with 2 and 50 μm sized latex beads, finding an adhesion force distribution with a mode of 11 ± 1 nN. This value corresponds well to the value presented here, taking into consideration the different aspects of the experimental protocols including differences in critical parameters such as loading rate, bead size, contact area and avidin coverage.

3.3. Detachment of beads using computer controlled micropipette – indirect adhesion force measurements

The adhesion force of the surface attached beads was also measured by CCMP. The size of the population probed in a run was chosen to be approximately 150. Since the duration of the measurement scales linearly with population size, there is a practical limit to the number of microparticles that can be measured. Taking into consideration the whole duration of an experiment, the throughput of the technique is approximately 2 particles per minute, which gives a sample size of N = 120 in an hour.

After the position of the particles is determined by computer vision, the glass micropipette with an inner diameter of 70 μm is moved over the beads one after the other and a negative pressure is applied above each bead for a certain amount of time (valve opening time, T). The principle of the measurement is illustrated in Fig. 3(a). The micropipette tip is kept at a distance of 10 μm from the surface during the measurement. The initial height setting is done by approaching the pipette to the sample surface in 1 μm steps and observing the mechanical vibrations of the tip visible in the microscope [40]. Vibrations stop when the micropipette tip touches the surface. In order to keep the distance between the surface of the dish and the micropipette throughout the measurement, a mathematical plane is fitted to the region of interest by the control software on the basis of optical focusing onto the four corners of the ROI. When the micropipette is traveling through the sample, its height is corrected using this plane, compensating any oblique positioning of the dish in the sample holder. This correction method provides an overall accuracy of ~2 μm in height, set by the depth of field of the objective lens. Once the entire pop-

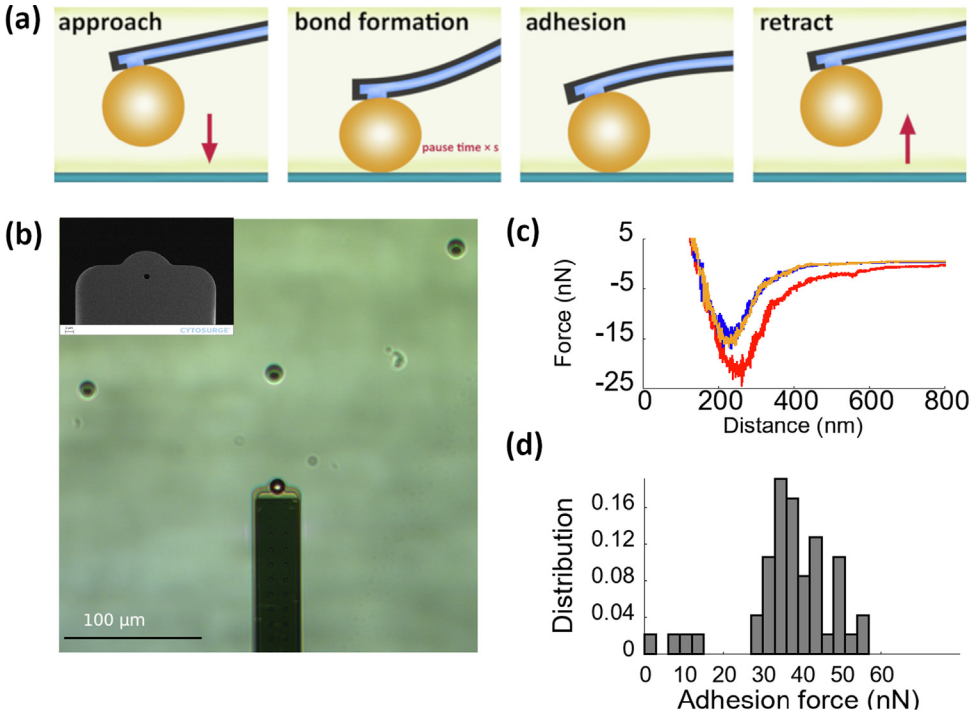

Fig. 2. (a) Schematics of the workflow of FluidFM colloid force spectroscopy. The cantilever with the bead attached is approached to the surface (first image), then it is let to adhere for a pre-set amount of time (second image). In the experiments presented here, pause time was set to 1 min. Afterwards, the cantilever is lifted up from the surface, and the adhesion causes a bending (third image). When the bonds are broken, the cantilever is fully retracted (fourth image). (b) Optical microscopy image of the experiment as seen on the screen of the FluidFM BOT. Three beads are visible on the image, while one bead is shown attached to the cantilever. The inlet shows a scanning electron microscope image of the tip, with the 2 μm aperture in the middle. (c) Typical force distance curves measured by FluidFM. (d) The adhesion force distribution measured on N = 47 beads from FluidFM colloid force spectroscopy. The mode of the adhesion force distribution with the standard error is 37.5 ± 1.8 nN.

ulation of beads has been visited, the negative pressure value in the pressure controller is increased and the pipette probes the remaining beads again. The number of such cycles is determined by the operator and can be adapted to the desired resolution of the adhesion force spectrum. If the negative pressure is increased in small steps, the force resolution of the method improves, however the measurement time will be longer due to the larger number of probing events. This tradeoff between the parameters has to be taken into consideration when planning experiments.

The valve opening time (T), which determines for how long the negative pressure and thus the flow and the hydrodynamic lifting force is applied to the bead is an important parameter. Detachment statistics of four separate measurements with different valve opening times are shown in Fig. 3(c). As the negative pressure is increased in every subsequent cycle, the number of remaining beads decreases accordingly. By taking the difference between the beads remaining in cycle N and N-1, a distribution can be measured. Such an adhesion distribution is shown in Fig. 3(b) with a mean of 6732.8 Pa as measured on a population of N = 253 beads. In this case, the valve opening time was set to 100 ms to match the timescale of the FluidFM bead detachment (shown in the inset of Fig. 3(b)). This is necessary in order to compare the histograms measured by the two methods.

The rate of the detachment of beads shows a dependence on the valve opening time, namely the longer the same negative pressure is applied, the more likely a bead detaches from the surface. This is further demonstrated in Fig. 3(d) where the detachment of beads is shown as a function of the valve opening time. The lines correspond to different values of negative pressure that is applied on the beads, essentially measuring the bond lifetime under constant force conditions. Consequently, the measurement principle of the CCMP experiments can be applied in two ways: it is possible to increase the pulling force in cycles with a constant valve opening time and to acquire an adhesion distribution from the data. Secondly, it is also possible to apply a consistent force on the beads and increase the valve opening time in the next cycle to determine the lifetime distribution of the multiple bond system under constant force. While the two measurement modes extract similar information, one or the other can be advantageous for certain applications.

The biochemical system used in the experiments provides the possibility to change the surface density of the biotin molecules, thus to modify the adhesion force of the beads. This can be achieved by mixing the PLL-*g*-PEG-biotin with PLL-*g*-PEG before the first surface treatment step. This way the surface density of the biotin is diluted leading to reduced adhesion. To demonstrate the ability of the CCMP to discriminate between different surface concentrations of the ligand as well as to examine unspecific binding, further experiments were performed. Four dilutions of PLL-*g*-PEG-biotin with PLL-*g*-PEG were prepared in the following ratios: 1:0 (pure PLL-*g*-PEG-biotin), 1:4, 1:16 and 0:1 (pure PLL-*g*-PEG). Subsequently, the glass surfaces were functionalized with each mixture and bead detachment experiments were executed using the same protocol. The results are presented in Fig. 4 for each surface, averaging three repeat experiments. Pure PLL-*g*-PEG does not induce adhesion as 98% of the beads detach after the first round of probing using the minimum picking force.

The correlation coefficient between the ratio of PLL-*g*-PEG-biotin and the mode detachment pressure is C = 0.9270 which

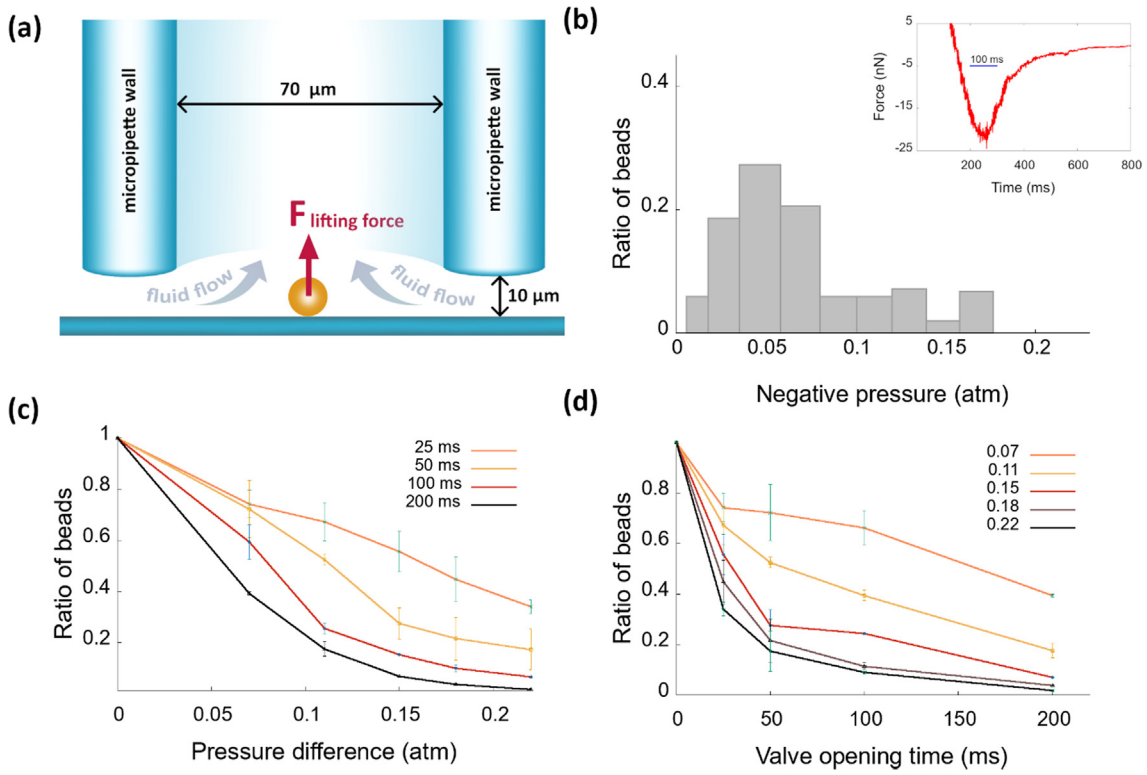

Fig. 3. Drawing of the micropipette tip with the bead underneath in a side view. The negative pressure induces an inwards fluid flow which in turn exerts a lifting force on the bead. The micropipette is kept at a constant distance of 10 µm from the surface. (b) Detachment pressure distribution measured by the micropipette with a valve opening time of 100 ms measured on N = 450 beads. The mode of the distribution is 4761 Pa. The valve opening time was chosen to match the timescale of the bead detachment process in the FluidFM. The inlet shows a typical force-time curve as measured by the FluidFM. (c) Detachment curves corresponding to different valve opening times. The ratio of beads remaining on the surface is shown as a function of the applied negative pressure. The error bars show the standard error of the mean of 3 independent measurements on separately prepared surfaces each on a sample of 150 beads. (d) Same data as presented on (c) but shown as a function of the valve opening time for the different applied negative pressure values given in atm. The error bars show the standard deviation of 3 independent measurements on separately prepared surfaces each on a sample of 150 beads.

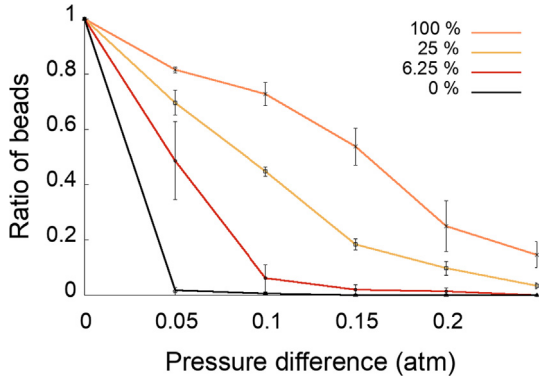

Fig. 4. Experiment showing the detachment of beads from surfaces with different ligand concentrations. Ratios of PLL-*g*-PEG-biotin to PLL-*g*-PEG in the surface treatment mixture is shown for each curve in the legend. There is a clear correlation between the strength of adhesion and the concentration of biotin on the surface. Error bars show the standard error of the mean of 3 independent measurements on separately prepared surfaces, each on a sample of 120 beads.

demonstrates that CCMP can determine the relative strength of molecular adhesion in a reproducible manner.

3.4. Comparison of distributions

For the validation of the adhesion force spectrum measured by the micropipette, a comparison of the data to the spectrum measured by FluidFM is needed. The results of two methods can only be realistically compared when the time scale of the bead detachment matches in both cases (Fig. 3(b)). In order to fulfill this condition, we used a valve opening time of 100 ms with CCMP and a loading rate of 200 nN/s in the FluidFM experiments. Since both measured histograms appear to be unimodal, we estimated that the modes of the distributions correspond to each other. Consequently, dividing the two numbers gives us a conversion value between the negative pressure measured by the micropipette and the adhesion force of the beads: $c = 797$ nN/atm. Fig. 5(b) shows the adhesion force spectrum of the bead population converted from the CCMP experiment (for comparison, the adhesion spectrum measured by the FluidFM is show in Fig. 5(a)). The differences mainly appear at the edges of the spectra which we attributed to the smaller sample size of the FluidFM measurement. (Duration of data acquisition was about the same (~2h) with both methods.)

According to our OWLS results, detachment of the beads is a consequence of the breakage of a large number of bonds loaded in a parallel way since the surface density of avidin is 70 ng/cm^2. The typical rupture force of a single avidin–biotin bond has been shown experimentally to be in the range of 160–200 pN [26,27] and values as high as 800 pN were proposed theoretically [41]. The exact value strongly depends on experimental conditions and on the loading rate, when measured by AFM. The loading rate has an impact on both the rupture force of a bond modeled with a single potential wall and in case of the streptavidin-biotin binding it also affects the pathway of the rupture through the multiple intermediate states [28]. The consequence of this dependence on the loading rate in case of a large set of parallel bonds is that the rupture force of an ensemble (F_m^*) is not quantized with the single bond rupture force (F_s^*). Instead, there is a transcendental mathematical relationship between F_m^* and N, from which the following inequality results [42]:

$$F_m^* < N \cdot F_s^* \quad (3)$$

Therefore, single bond rupture force values cannot be acquired in this way, just as the overall detachment force cannot be determined by knowing the rupture force of a single bond.

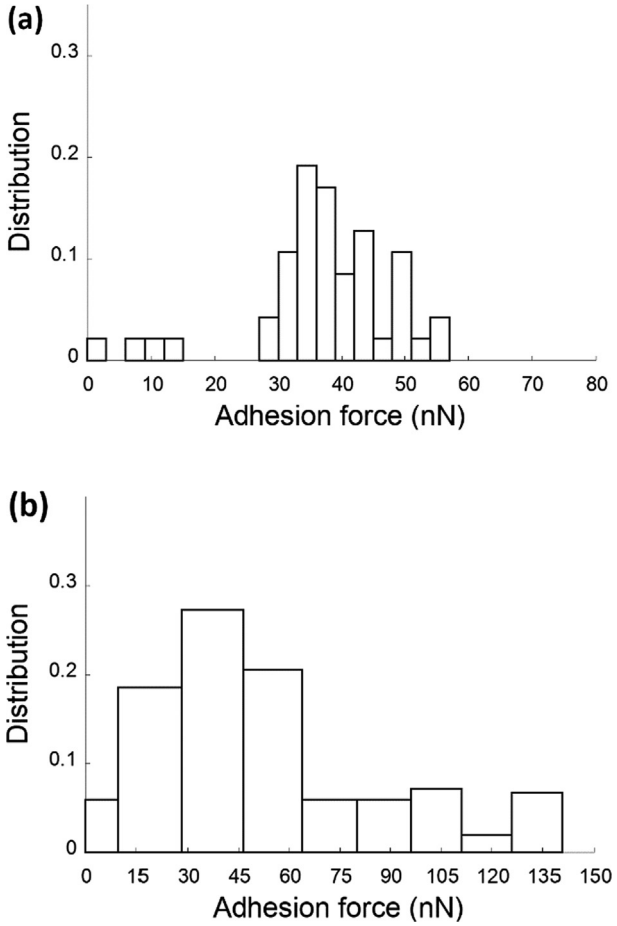

Fig. 5. (a) Normalized adhesion force distributions of beads measured by the FluidFM (N = 47, mode of the force distribution with standard error given is 37.5 ± 1.8 nN). (b) Normalized adhesion force distribution measured by CCMP with a valve opening time of 100 ms. The negative pressure values were converted to force by setting the mode of the spectrum to the mode of the FluidFM results.

To give an estimate of F_s^*, the number of avidin-biotin bonds participating in the adhesion of beads in our experiments was estimated from the contact area of the beads and the surface density measured by the OWLS method. In our case, using the formula of JKR theory [43] as well as considering the gyration radius of the PLL-*g*-PEG chains [44], we acquire a contact area of $A = 1.5 \cdot 10^{-14}$ m^2 which amounts to 100 avidin molecules under the beads. Therefore a limit value of $F_s^* = 188 - 375$ pN is given, depending on how many of the available binding pockets of the avidin molecules is occupied by a biotin on average.

4. Conclusions

In this study we applied a novel method, the computer controlled micropipette (CCMP), for measuring the adhesion force histogram of several hundreds of functionalized microparticles. The combined throughput and available force range of the technique potentially opens up new possibilities in surface and colloid sciences and related applications. The CCMP method directly determines the negative pressure difference that can detach an individual particle from the surface. In order to calibrate this pressure difference value to a detachment force, a model-system was established using 10 μm polystyrene beads immobilized on the surface through the well-characterized biotin-avidin linkage. The in situ build-up of the molecular surface layers and the subsequent

adsorption of the beads was revealed by optical waveguide lightmode spectroscopy (OWLS). The microparticle adhesion spectrum was directly measured by colloid force spectroscopy using the novel robotic fluidic force microscopy method (FluidFM BOT) then compared to the spectrum deduced from micropipette experiments. The adhesion force distribution was determined and the mode was found to be $F = 37.5 \pm 1.8$ nN, similar to what has been determined earlier using a comparable chemical system [30].

The two methodologies allowed us to determine the adhesion force distribution of the attached beads, making a quantitative comparison possible. We find that the two adhesion force histograms can be reasonably correlated which opens the way towards accurate detachment force measurements of any microparticle system by the novel CCMP method. Two measurement modes are proposed in further CCMP experiments: (*i*) recording the detachment force using a consistent valve opening time, and (*ii*) measuring the bond lifetime under constant applied force. Either of these modes have a higher throughput than traditional colloid force microscopy methods or even FluidFM when measuring the adhesion force on populations of microbeads. Namely, a measurement speed of 2 beads per minute can be reached routinely with the micropipette, including the preparation time of the setup. The maximal applicable lifting force amounts to several micronewtons as it is only limited by the highest value of pressure difference that can be applied without destabilizing the sample. By varying the composition of the surface treatment we demonstrated that the CCMP method is capable of differentiating bead populations depending on their adhesion strength, thus characterizing the effect of coatings on microparticle attachment.

The micropipette based method has been used for characterizing live cell adhesion earlier [40,45], however here we present the first instance of a calibrated force adhesion spectrum measurement on microparticles. The technique can be easily adapted for any particle size by adjusting the inner diameter of the micropipette accordingly down to around 1 μN in bead size. The material composition of the beads does not influence the measurement; therefore, a wide variety of samples can be probed. It is important to highlight that the force range is readily adaptable, with forces up to several micronewtons attainable. Further work is under way to develop and calibrate an accurate single-cell level cell adhesion assay and to apply it on biologically interesting cell populations. Based on the results, we also envision the applicability of CCMP technology to measure the adhesion of bacteria to functionalized surfaces in order to characterize bacteria repellent or adhesive coatings.

In the future, we expect that the introduced methodologies will find widespread applications in the study of surface interactions both for basic and applied research. Especially those areas can benefit where large amount of adhesion data has to be obtained in a reasonable time frame, in a straightforward and automatized manner. For example, characterizing heterogeneity in adsorbing surfaces or in adsorbing colloidal objects, optimizing surface adhesion, surface cleaning protocols of electronics materials such as silicon wafers [46] and relevant coatings for industrial and basic research applications. Furthermore, the different modes of measurement can be later used to gain information on the energy landscape of molecular bonds.

Acknowledgements

This work was supported by the following funding programs: ÚNKP-18-3 New National Excellence Program of the Ministry of Human Capacities, Lendület (MTA), KKP_19 (NKFIH), KH_17 (NKFIH) and ERC_HU (NKFIH)).

Appendix A. Supplementary material

Supplementary data to this article can be found online at https://doi.org/10.1016/j.jcis.2019.07.102.

References

[1] M.A.S. Quintanilla, A. Castellanos, J.M. Valverde, Correlation between bulk stresses and interparticle contact forces in fine powders, Phys. Rev. E - Stat. Physics, Plasmas, Fluids, Relat. Interdiscip. Top. (2001), https://doi.org/10.1103/PhysRevE.64.031301.
[2] W.R. Bowen, R.W. Lovitt, C.J. Wright, Atomic force microscope studies of stainless steel: Surface morphology and colloidal particle adhesion, J. Mater. Sci. (2001), https://doi.org/10.1023/A:1004864219379.
[3] M. Holmberg, R. Wigren, R. Erlandsson, P.M. Claesson, Interactions between cellulose and colloidal silica in the presence of polyelectrolytes, Colloids Surfaces A Physicochem. Eng. Asp. (1997), https://doi.org/10.1016/S0927-7757(97)00036-8.
[4] M. Kappl, H.-J. Butt, The colloidal probe technique and its application to adhesion force measurements, Part. Part. Syst. Char. 19 (2002) 129–143, https://doi.org/10.1002/1521-4117.
[5] Z. Adamczyk, M. Nattich, M. Wasilewska, M. Sadowska, Deposition of colloid particles on protein layers: Fibrinogen on mica, J. Colloid Interface Sci. 356 (2011) 454–464, https://doi.org/10.1016/j.jcis.2011.01.009.
[6] M. Fuji, K. Machida, T. Takei, T. Watanabe, M. Chikazawa, Effect of wettability on adhesion force between silica particles evaluated by atomic force microscopy measurement as a function of relative humidity, Langmuir (1999), https://doi.org/10.1021/la981533c.
[7] M. Giesbers, J.M. Kleijn, G.J. Fleer, M.A. Cohen Stuart, Forces between polymer-covered surfaces: A colloidal probe study, Colloids Surfaces A Physicochem. Eng. Asp. (1998), https://doi.org/10.1016/S0927-7757(98)00366-5.
[8] M. Borkovec, I. Szilagyi, I. Popa, M. Finessi, P. Sinha, P. Maroni, G. Papastavrou, Investigating forces between charged particles in the presence of oppositely charged polyelectrolytes with the multi-particle colloidal probe technique, Adv. Colloid Interface Sci. (2012), https://doi.org/10.1016/j.cis.2012.06.005.
[9] R. Schröder, J. Schmidt, S. Blättermann, L. Peters, N. Janssen, M. Grundmann, W. Seemann, D. Kaufel, N. Merten, C. Drewke, J. Gomeza, G. Milligan, K. Mohr, E. Kostenis, Applying label-free dynamic mass redistribution technology to frame signaling of G protein-coupled receptors noninvasively in living cells, Nat. Protoc. 6 (2011) 1748–1760, https://doi.org/10.1038/nprot.2011.386.
[10] P. Kanchanawong, G. Shtengel, A.M. Pasapera, E.B. Ramko, M.W. Davidson, H.F. Hess, C.M. Waterman, Nanoscale architecture of integrin-based cell adhesions, Nature 468 (2010) 580–584, https://doi.org/10.1038/nature09621.
[11] S. Sabri, M. Soler, C. Foa, A. Pierres, A. Benoliel, P. Bongrand, Glycocalyx modulation is a physiological means of regulating cell adhesion, J. Cell Sci. (2000).
[12] R. Ungai-Salánki, B. Peter, T. Gerecsei, N. Orgovan, R. Horvath, B. Szabó, A practical review on the measurement tools for cellular adhesion force, Adv. Colloid Interface Sci. (2019), https://doi.org/10.1016/j.cis.2019.05.005.
[13] F. Podczeck, J.M. Newton, M.B. James, Influence of relative humidity of storage air on the adhesion and autoadhesion of micronized particles to particulate and compacted powder surfaces, J. Colloid Interface Sci. (1997), https://doi.org/10.1006/jcis.1996.4684.
[14] F. Podczeck, J.M. Newton, M.B. James, Assessment of adhesion and autoadhesion forces between particles and surfaces, J. Adhes. Sci. Technol. (1994), https://doi.org/10.1163/156856194x00744.
[15] B. Angres, A. Barth, W.J. Nelson, Mechanism for transition from initial to stable cell-cell adhesion: Kinetic analysis of E-cadherin-mediated adhesion using a quantitative adhesion assay, J. Cell Biol. (1996), https://doi.org/10.1083/jcb.134.2.549.
[16] E. Martines, K. McGhee, C. Wilkinson, A. Curtis, A Parallel-plate flow chamber to study initial cell adhesion on a nanofeatured surface, IEEE Trans. Nanobiosci. 3 (2004) 90–95, https://doi.org/10.1109/TNB.2004.828268.
[17] J. Helenius, C.-P. Heisenberg, H.E. Gaub, D.J. Muller, Single-cell force spectroscopy, J. Cell Sci. (2008), https://doi.org/10.1242/jcs.030999.
[18] G. Sagvolden, I. Giaever, E.O. Pettersen, J. Feder, Cell adhesion force microscopy, Proc. Natl. Acad. Sci. U. S. A. 96 (1999) 471–476, https://doi.org/10.1073/pnas.96.2.471.
[19] D. Kamsma, G.J.L. Wuite, Single-molecule measurements using acoustic force spectroscopy (AFS). In: Methods Mol. Biol., 2018. doi: 10.1007/978-1-4939-7271-5_18.
[20] M. Marchetti, D. Kamsma, E. Cazares Vargas, A. Hernandez Garcia, P. van der Schoot, R. de Vries, G.J.L. Wuite, W.H. Roos, Real-time assembly of an artificial virus elucidated at the single-particle level, BioRxiv. (2019), https://doi.org/10.1101/526046 526046.
[21] G. Bergamaschi, A. Biebricher, G.J.L. Wuite, From nuclei to artificial cells: probing the mechanics of minimal systems, Biophys. J. 116 (2019) 123a, https://doi.org/10.1016/j.bpj.2018.11.687.
[22] D. Kamsma, P. Bochet, F. Oswald, N. Alblas, S. Goyard, G.J.L. Wuite, E.J.G. Peterman, T. Rose, Single-cell acoustic force spectroscopy: resolving kinetics and strength of T cell adhesion to fibronectin, Cell Rep. 24 (2018) 3008–3016, https://doi.org/10.1016/j.celrep.2018.08.034.
[23] D. Leckband, The surface apparatus–a tool for probing molecular protein interactions, Nature 376 (1995) 617–618, https://doi.org/10.1038/376617a0.

[24] J.N. Israelachvili, P.M. McGuiggan, Adhesion and short-range forces between surfaces. part I: New apparatus for surface force measurements, J. Mater. Res. 5 (1990) 2223–2231, https://doi.org/10.1557/JMR.1990.2223.
[25] E. Evans, Looking inside molecular bonds at biological interfaces with dynamic force spectroscopy, Biophys. Chem. 82 (1999) 83–97, https://doi.org/10.1016/S0301-4622(99)00108-8.
[26] V.T. Moy, E.L. Florin, H.E. Gaub, Adhesive forces between ligand and receptor measured by AFM, Colloids Surfaces A Physicochem. Eng. Asp. 93 (1994) 343–348, https://doi.org/10.1016/0927-7757(94)02933-4.
[27] R.S. Pillai, S.N. Bhattacharyya, C.G. Artus, T. Zoller, N. Cougot, E. Basyuk, E. Bertrand, W. Filipowicz, Adhesion forces between individual ligand-receptor pairs, Nature 20 (1994) 493–494, https://doi.org/10.1038/020493a0.
[28] F. Rico, A. Russek, L. Gonzalez, H. Grubmuller, S. Scheuring, Heterogeneous and rate-dependent streptavidin-biotin unbinding revealed by high-speed force spectroscopy and molecular dynamics simulations, PNAS 116 (2019) 6594–6596, https://doi.org/10.1073/pnas.1816909116.
[29] A. Meister, M. Gabi, P. Behr, P. Studer, J. Vörös, P. Niedermann, J. Bitterli, J. Polesel-Maris, M. Liley, H. Heinzelmann, T. Zambelli, FluidFM: Combining atomic force microscopy and nanofluidics in a universal liquid delivery system for single cell applications and beyond, Nano Lett. 9 (2009) 2501–2507, https://doi.org/10.1021/nl901384x.
[30] P. Dörig, D. Ossola, A.M. Truong, M. Graf, F. Stauffer, J. Vörös, T. Zambelli, Exchangeable colloidal AFM probes for the quantification of irreversible and long-term interactions, Biophys. J. 105 (2013) 463–472, https://doi.org/10.1016/j.bpj.2013.06.002.
[31] N. Helfricht, A. Mark, L. Dorwling-Carter, T. Zambelli, G. Papastavrou, Extending the limits of direct force measurements: Colloidal probes from sub-micron particles, Nanoscale 9 (2017) 9491–9501, https://doi.org/10.1039/c7nr02226c.
[32] A. Saftics, B. Türk, A. Sulyok, N. Nagy, T. Gerecsei, I. Szekacs, S. Kurunczi, R. Horvath, Biomimetic dextran-based hydrogel layers for cell micropatterning over large areas using the FluidFM BOT technology, Langmuir 35 (2019) 2412–2421, https://doi.org/10.1021/acs.langmuir.8b03249.
[33] J.E. Sader, Calibration of atomic force microscope cantilevers, 70 (2002) pp. 846–856.
[34] Z. Környei, S. Beke, T. Mihálffy, M. Jelitai, K.J. Kovács, Z. Szabó, B. Szabó, Cell sorting in a Petri dish controlled by computer vision, Sci. Rep. 3 (2013), https://doi.org/10.1038/srep01088.
[35] N. Sándor, S. Lukácsi, R. Ungai-Salánki, N. Orgován, B. Szabó, R. Horváth, A. Erdei, Z. Bajtay, CD11c/CD18 dominates adhesion of human monocytes, macrophages and dendritic cells over CD11b/CD18, PLoS ONE 11 (2016) 1–17, https://doi.org/10.1371/journal.pone.0163120.
[36] E. Farkas, D. Srankó, Z. Kerner, B. Setner, Z. Szewczuk, W. Malinka, R. Horvath, Ł. Szyrwiel, J.S. Pap, Self-assembled, nanostructured coatings for water oxidation by alternating deposition of Cu-branched peptide electrocatalysts and polyelectrolytes, Chem. Sci. (2016), https://doi.org/10.1039/c6sc00595k.
[37] N. Orgovan, D. Patko, C. Hos, S. Kurunczi, B. Szabó, J.J. Ramsden, R. Horvath, Sample handling in surface sensitive chemical and biological sensing: A practical review of basic fluidics and analyte transport, Adv. Colloid Interface Sci. (2014), https://doi.org/10.1016/j.cis.2014.03.011.
[38] J. Vörös, The density and refractive index of adsorbing protein layers, Biophys. J. (2004), https://doi.org/10.1529/biophysj.103.030072.
[39] J.J. Ramsden, R. Horvath, Optical biosensors for cell adhesion, J. Recept. Signal Transduct. 29 (2009) 211–223, https://doi.org/10.1080/10799890903064119.
[40] R. Salánki, C. Hős, N. Orgovan, B. Péter, N. Sándor, Z. Bajtay, A. Erdei, R. Horvath, B. Szabó, Single cell adhesion assay using computer controlled micropipette, PLoS ONE 9 (2014), https://doi.org/10.1371/journal.pone.0111450 e111450.
[41] S. Izrailev, S. Stepaniants, M. Balsera, Y. Oono, K. Schulten, Molecular dynamics study of unbinding of the avidin-biotin complex, Biophys. J. 72 (1997) 1568–1581, https://doi.org/10.1016/S0006-3495(97)78804-0.
[42] P.M. Williams, Analytical descriptions of dynamic force spectroscopy: Behaviour of multiple connections, Anal. Chim. Acta 479 (2003) 107–115, https://doi.org/10.1016/S0003-2670(02)01569-6.
[43] L.C. Xu, B.E. Logan, Interaction forces between colloids and protein-coated surfaces measured using an atomic force microscope, Environ. Sci. Technol. 39 (2005) 3592–3600, https://doi.org/10.1021/es048377i.
[44] G.L. Kenausis, J. Vörös, D.L. Elbert, N. Huang, R. Hofer, L. Ruiz-Taylor, M. Textor, J.A. Hubbell, N.D. Spencer, Poly(L-lysine)-g-Poly(ethylene glycol) layers on metal oxide surfaces: attachment mechanism and effects of polymer architecture on resistance to protein adsorption †, J. Phys. Chem. B (2000), https://doi.org/10.1021/jp993359m.
[45] N. Orgovan, R. Salánki, N. Sándor, Z. Bajtay, A. Erdei, B. Szabó, R. Horvath, In-situ and label-free optical monitoring of the adhesion and spreading of primary monocytes isolated from human blood: Dependence on serum concentration levels, Biosens. Bioelectron. 54 (2014) 339–344, https://doi.org/10.1016/j.bios.2013.10.076.
[46] M.B. Ranade, Adhesion and removal of fine particles on surfaces, Aerosol Sci. Technol. 7 (1987) 161–176, https://doi.org/10.1080/02786828708959155.